

MODELLING OF MICROSTRUCTURAL CREEP DAMAGE IN WELDED JOINTS
OF 316 STAINLESS STEEL

G.Bouche*, L.Allais**, V.Lezaud**, R.Piques*, A.Pineau*

The present work has been undertaken to model creep damage in welded joints. The complex dual phase microstructure of 316L welds are simulated by manually filling a mould with longitudinally deposited weld beads. Columnar grains of austenite constitute a matrix in which thin dendrites of δ -ferrite can be found. The material was then aged for 2000 hours at 600°C. This ageing heat treatment generates the precipitation of chromium carbides and the reduction in δ ferrite.

Smooth and notched creep specimens were cut from the mould and tested at 600°C under various stress levels. Notched specimens were calculated by finite elements method. Microstructural observations reveal that creep cavities are preferentially located along the austenite grain boundaries. The analysis of intergranular damage measured on cross sections of notched specimens is conducted to obtain a predictive damage law which could be used to estimate the lifetime of welded joints.

INTRODUCTION

The present work investigates creep damage in welded joints of 316L stainless steel, using a local approach which has proved to be efficient in a similar study on the base 316 material (1, 2). In a previous study, it was shown that a defect assessment method which used a global approach based on fracture mechanics failed in giving correct initiation time predictions in the case of welded joints (3). The objective of the present study is to obtain a predictive damage law based on the measurement of physical damage (cavities, intergranular cracks) in the case of the weld metal. Viscoplastic numerical simulations are developed for modelling the behaviour of the material and the best fit creep damage law. Since the stress-strain field can then be calculated in a component under service-like conditions, the damage criteria obtained will be directly used to evaluate the lifetime of the component. The present paper deals with the characterization of the microstructure, the identification and the modelling of the creep damage in such materials.

* Centre des Matériaux, Ecole des Mines de Paris, UMR CNRS 7633, BP87 91003 Evry, France

** Commissariat à l'Energie Atomique CEREM/Service de Recherches Métallurgiques Appliquées, Centre d'étude de Saclay, 91191 Gif sur Yvette Cedex, France

MATERIAL: COMPOSITION AND PROCESSING

Composition and preparation

The composition of the filling metal used for the welded joints under investigation is a 316L(N) type 19Cr-12Ni-2Mo stainless steel. The composition of the material is close to that of the fully austenitic base metal except that the balance between γ and δ -ferrite stabilizing elements was chosen to result in 5% to 10% ferrite in the weld. Since it is difficult to cut specimens for testing from an X weldment, a block was fabricated using the manual filling metal arc technique. The microstructure of 316L(N) welds was simulated by manually filling a mould with 82 longitudinal deposited weld beads. Specimens for the study have been cut along the three main directions (transverse, longitudinal and short transverse directions) of the mould for smooth specimens, and along the transverse direction only for notched specimens, since this orientation corresponds to the main loading direction in the components.

Microstructure and ageing of the material

Bead deposition results in the formation of a complex dual phase ($\gamma+\delta$) material in which austenite γ is the dominant phase. The austenite is organized into long grains of several millimeters in length along a direction close to the short transverse direction and approximately 50 to 100 μm in the cross section. Grains are oriented by both the thermal solidification gradient and fluid mechanics in the weld pool during welding (4). The second phase is residual ferrite δ . A fully austenitic material should be obtained at equilibrium for this composition. This presence of skeletal ferrite is due to the rapid solidification of the weld, comparable to a quench. Thin dendrites (1 μm thick) of ferrite can be observed inside and between austenite grains sharing the same orientation. As a consequence of the quench-like solidification of the weld beads, the material is unstable. At high temperature, it is not possible to dissociate the effect of ageing and the creep phenomena. Hence, in order to simulate creep phenomena occurring in service, the decision was made to carry out creep mechanical tests using specimens taken from the mould after ageing 2000 hours at 600°C. Ageing of the material has been experimentally studied. The evolution of the percentage of ferrite transformed while ageing the material at 600°C is presented in Figure 1. The description of the experiment and comparison with literature (5) have already been reported (6).

EXPERIMENTAL PROCEDURE AND RESULTS

Experimental procedure

Smooth and notched creep specimens were cut from the mould. The nominal stress applied to the smooth creep specimens tested at 600°C was in the range between 150 MPa to 210 MPa. These tests were carried out to obtain the behaviour of the material for numerical computations. Anisotropy of the material was also investigated.

Notched specimens were also tested to study creep damage. Two geometries, FLE 1-6 and FLE 4-6, which differ in notch-root radius R (1 and 4 mm, respectively) were used in order to have a wide range of stress triaxiality ratio in the specimen during the tests. In the notched section the mean stress range (270-290 MPa for the FLE 4-6 and 310-330 MPa for the FLE 1-6) was chosen to have tests which lasted approximately 1000 hours.

The tests were generally interrupted before failure to avoid final rupture. Longitudinal sections were extracted from the notch region and observed after etching and polishing several times, using both optical microscopy and SEM in order to reveal the damage.

Creep tests results

For the unaged material, results on creep tests, fracture analysis and hypotheses to explain the observed anisotropic behaviour of the material have been reported elsewhere (6). Results are similar on aged material with transverse specimens presenting a better resistance to creep than longitudinal specimens, and longitudinal better than short transverse. The main point of interest here consists, for the modelling aspect, of the experimental *elongation-time* curves for transverse smooth specimen creep tested at 600°C, for loads ranging from 150 MPa to 210 MPa. These curves were used for the identification of the constitutive laws. The notched specimens were devoted to the study of damage.

Damage analysis

Sections were made in the notched specimens to evaluate creep damage. Small cavities of diameter 1 μm to 20 μm can be observed (cf Fig. 2). Electrolytic etching with oxalic acid solution shows that damage can be located with respect to the microstructure using polarized light optical microscopy. Cavities and ferrite appear bright white while the austenitic matrix is colored (grey). Contrast between austenite grains, due to difference in orientation, can be observed. Cavities are located along the interfaces between austenite grains. Trying to locate cavities with respect to the ferrite has not been possible due to the small thickness of ferrite dendrites and the lack of resolution. Therefore, creep damage in 316L(N) welded joints is considered to be predominantly located at the γ - γ interfaces. Measurements of damage are then made using image analysis techniques on axial sections of creep tested notched specimens. The damage values are implemented into a model in order to find a relationship between the damage and the stress-strain fields obtained from the calculations.

NUMERICAL CALCULATIONS

Constitutive law identification

As described in the introduction, the objective of the study is to derive a predictive law for the development of creep damage in a welded joint and a criteria on admissible damage. An attempt will be made to develop a model similar to that used for the base

material (2). Using the curves *elongation versus time* for transverse smooth transverse specimens creep tested at nominal stress ranging from 150 MPa to 210 MPa, primary and secondary creep laws can be identified.

The third stage of creep is not modelled, being of less interest from the industrial point of view when considering that the structure is already extremely damaged at this point. Moreover tertiary creep in these materials is essentially of a structural nature. Simple power laws have been chosen :

$$(1) \quad \text{primary creep: } \varepsilon = C_1 \sigma^{n_1} t^{C_2}$$

$$(2) \quad \text{secondary creep: } \dot{\varepsilon} = C \sigma^n$$

A first set of coefficients has been manually identified. Then the software SIDOLO (7) was used to optimize this set. The value of n obtained is 9.75.

n characterizes the dependance of secondary creep rate towards stress. This value is close to the value of 7.69 obtained for the base material (2) and only half this value from a first identification conducted on the weld unaged material.

Calculation

With the code CASTEM 2000 (8), developed at CEA, the mechanical parameter fields are calculated for the notched specimens under creep loading. Given the symmetry of the specimen, only one quarter of the notched part is simulated.

The creep behaviour of a notch specimen is simulated in two parts : first an elastoplastic calculation is conducted to reach the nominal stress applied during creep test. The elastoplastic calculation is based on the value of E, ν , and on the experimental tensile curve. The result of this calculation is then used as the input for the creep test.

DISCUSSION

Figure 3 presents the result of redistribution with the time of the maximum principal stress in the minimum section of the specimens FLE1-6 and FLE4-6. Such a result had also been obtained for the base material (2). The maximum principal stress reaches its peak in the center of the minimum section for the 4 mm notch, whereas it is maximum close to the notch for the FLE1-6 at the time considered (about 1000 hours). This means that the effect of maximum principal stress, compared to creep strain, on damage appearance can be studied and quantified.

The first observations made on the longitudinal sections of a notched specimen show the damage is predominantly located in the middle of the minimum section for a FLE4-6. This highlights the effect of maximum principal stress on damage. A damage law is being identified. The last results concerning the location of damage in the minimum section of the notched specimens makes it reasonable to suggest the use of the incremental damage law : $dD = A \langle \Sigma \rangle^\alpha \varepsilon_{eqc}^\beta d\varepsilon_{eqc}$ defined by Piques (2) for the base metal since the behaviours of base and weld metal appear very similar. In this law, dD is the increment of intergranular damage, $\langle \Sigma \rangle$ is the principal stress, ε_{eqc}^β is the equivalent creep strain and $d\varepsilon_{eqc}$ its increment.

CONCLUSIONS

Although further mechanical testing must be completed on the aged material to be able to identify a damage law, some preliminary conclusions can already be drawn. They are presented here by increasing order of interest:

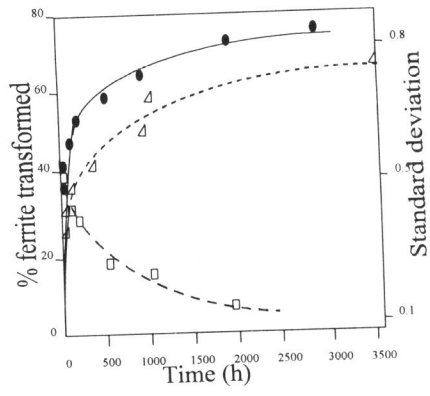
- (1) The microstructure of the weld metal is unstable and complex compared to that of the base metal.
- (2) The consequences of ageing of the weld metal at 600°C must be taken into account. The weld material was aged for 2000 hours at 600°C to develop a more stable microstructure.
- (3) The behaviour of the weld material under creep loading is anisotropic (6).
- (4) In secondary creep stage, the exponent of the dependence of creep deformation rate towards stress is close to the one identified for the base metal 316L(N) ($n = 7.69$).
- (5) Creep cavitation is essentially located at the austenite-austenite interfaces. This last result is consistent with previous results reported on the base metal (2). Hence, the first attempt of damage modelling will be done using an incremental law similar to the one used in that study.

ACKNOWLEDGEMENTS

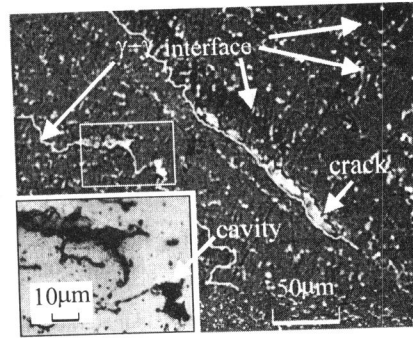
M.Simoes and F.Grillon are greatly acknowledged for their help in the SEM observations and analysis and A. Laurent for her technical support.

REFERENCES

- (1) Yoshida M et al, Mechanical Engineering Publications Limited, Edited by P.Bensussan and J.P. Mascarell, EGF Publication 6, 1990, pp. 3-21.
- (2) Piques R., PhD thesis, Ecole des Mines de Paris, 1989.
- (3) Allais et al, accepted in *Fatigue & Fracture of Eng. Mat. & Struct.*
- (4) Institut de soudure, Rapport DGRST N°71.7.2789, 1971.
- (5) Mathew M.D et al, *Mat. Science & Tech.*, Vol.7, 1991, pp. 533-535.
- (6) Bouche G et al, *Hida Conference Proceedings*, W6, 1998.
- (7) SIDOLO , notice d'utilisation, version 2.3, ENSMP, 1984.
- (8) CASTEM 2000 , manuel d'utilisation, rapport CEA/SEMT, 1995.



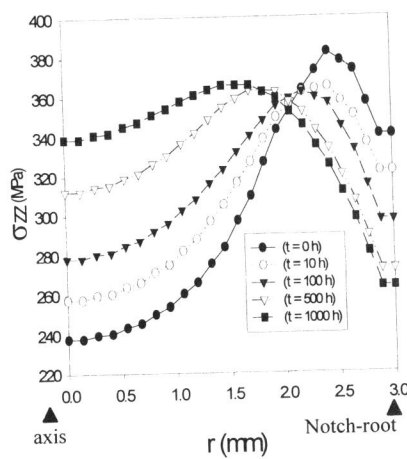
- Δ - % ferrite transformed Mathew et al (5)
 - \bullet - % ferrite transformed present study
 - \square - standard deviation



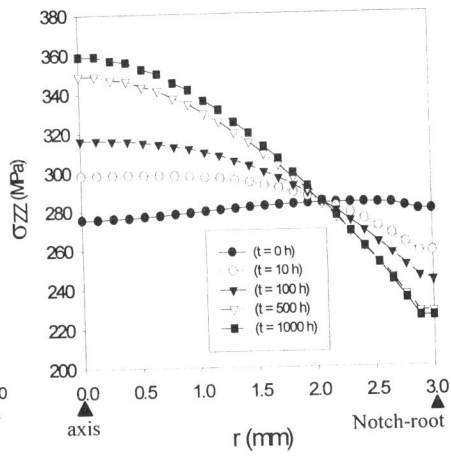
(some γ - γ interfaces are highlighted)

Figure 1 Evolution of the % of ferrite transformed during ageing at 600°C

Figure 2 Micrograph of the microstructure and damage analysis



Notch-root radius = 1mm



Notch-root radius = 4 mm

Figure 3 Redistribution of the maximum principal stress in the minimum section of the notched specimens, results of F.E.M. calculations: a) R=1mm b) R=4mm